Characterization of the Structure of a Novel Refractory Alloy Glass – $Ni_{60}Nb_{37}Sn_3$

Michelle L. Tokarz[1], Matt Daniels[1], John C. Bilello[1], Zofia Rek[2]
[1]Center for Nanomaterials Science, Department of Materials Science and Engineering; University of Michigan, Ann Arbor, MI 48109
[2]Stanford Synchrotron Radiation Laboratory; Stanford University, Menlo Park, CA 94025

ABSTRACT

Bulk forms of Refractory Alloy Glasses (RAGs) of the composition $Ni_{60}Nb_{37}Sn_3$ have recently been synthesized as part of a larger project for potential use in structural applications. Modeling efforts of such metallic glasses have traditionally involved the use of hard sphere models without regard to potential electron density fluctuations of individual components. X-ray characterization of these materials (in both reflection and transmission modes) provided scattering data necessary for subsequent radial distribution analysis, which gives structural information such as nearest neighbor distances and packing characteristics. A model radial distribution function (RDF) was constructed based upon a hard sphere space filling assumption and compared to the RDFs obtained from experimental scattering data. The experimental RDFs showed no difference from the model RDF within the limit of experimental error, with regard to nearest neighbor distances and coordination numbers of the first two nearest neighbors.

Additionally, transmission mode scattering experiments from a white beam x-ray source (E = 2 to 40 keV) demonstrated a through thickness amorphous structure of 2mm thick samples. Converted line profiles from the two-dimensional diffraction patterns from this experiment also showed agreement with reflection mode experiments. Samples of Vitreloy-106 ($Zr_{57}Nb_5Cu_{15.4}Ni_{12.6}Al_{10}$) of similar thicknesses were used as standards due to the well-known behavior of this particular class of metallic glasses.

INTRODUCTION

Some of the initial glassy metals were formed by a method called splat cooling [1,2] whereby the constituents were induction melted under an Ar atmosphere and then catapulted onto a cooled surface. This method produced ribbons with typical thickness of 40-60 μm. More recently, Johnson and Duwez and coworkers began producing bulk (thicknesses up to 3 mm) metallic glasses [3]. These glasses are generally multicomponent alloy systems that are characterized by deep eutectics and large differences in atomic sizes and atomic numbers. When these materials are cooled fast enough, the thermodynamically favored eutectic structure is bypassed to form the kinetically favored glass.

Metallic glasses are of interest due to their potential for increased stiffness. Because of their amorphous structure, they have no slip planes to aid in yielding processes. Additionally, the bulk metallic glasses mentioned above have been quoted to have critical cooling rates for glass formation on the order of 1 K/s as opposed to monatomic metals which can have critical cooling rates up to 10^9 K/s [4]. This allows for reasonable processing methods such as injection molding for near net-shaped parts. Potential applications of these materials range as widely as golf clubs to automobile engine components.

However, these materials can be plagued by high brittleness as is characteristic of many glasses. During processing, the difference in heating rates through the thickness can result in

high strain gradients, ultimately leading to brittleness. Additionally, these materials tend to crystallize at elevated temperatures, limiting their use to lower temperature applications.

Finally, the amorphous nature of these glasses complicates the fundamental understanding of their structure due to the inability to use classical scattering methods as used for crystalline materials. They do not exhibit defined diffraction peaks and subsequently raw scattering data cannot be used quantitatively for characterization. Additionally, to date only reflection mode scattering experiments have been performed on bulk metallic glasses. Thus there is no information about the "bulk" structure. (Attenuations lengths for typical reflection mode x-ray scattering experiments tend to be less than 10μm).

Thus, while the potential properties and applications of bulk metallic glasses are very attractive, they also present some unique challenges.

Recent efforts have focused on a new class of bulk metallic glasses called Refractory Alloy Glasses (RAGs). The goal in using these materials is to take advantage of the higher melting points of the constituents to give higher phase transition temperatures and thus better stabilities. This paper will specifically focus on the $Ni_{60}Nb_{37}Sn_3$ system. (Tm_{Ni} = 1455 °C, Tm_{Nb} = 2477 °C, Tm_{Sn} = 232 °C)

EXPERIMENTAL DETAILS

Two bulk metallic glasses were studied, Vitreloy-106 and the $Ni_{60}Nb_{37}Sn_3$ RAG mentioned above. While the Vitreloy-106 samples were used as standards, the RAG samples were of main concern.

The syntheses of these materials [5] were conducted by an arc melting of the constituents in the amounts necessary to produce the chemical composition desired. These melts were cooled into ingots and remelted to 850 - 1100 °C in vacuum. Finally they were injected into copper molds and cooled to ambient. These molds produced samples that were nominally 30mm x 6mm x 2mm.

Characterization of these materials consisted of x-ray scattering in reflection and transmission modes. Transmission mode scattering was performed with a synchrotron white-beam x-ray source (E = 2 to 40 KeV) in conjunction with a pin-hole slit which allowed for near point source optics. Resulting diffraction images were captured on exposed Polaroid film. These films were inverted and subsequent line profiles were taken and converted to classical Intensity vs. 2θ plots. Finally, for comparison to other experiments, these data were converted to sin θ / λ plots via weighted averages of the percentages of energies transmitted through the sample.

Reflection mode scattering was accomplished with two different experimental setups. The first of these was a synchrotron monochromatic beam source (λ=1.23 Å) with an incident angle θ = 3°. The second was a lab source rotating anode ($Cu_{k\alpha}$, λ=1.54 Å) with an incident angle θ = 2° and a scintillation counter detector. (At these incident angles and energies, attenuations lengths were less than 10 μm.)

Radial distribution analysis was performed via methods outlined by Warren [6] and using software written by Petkov [7].

RESULTS AND DISCUSSION

Transmission Mode Scattering

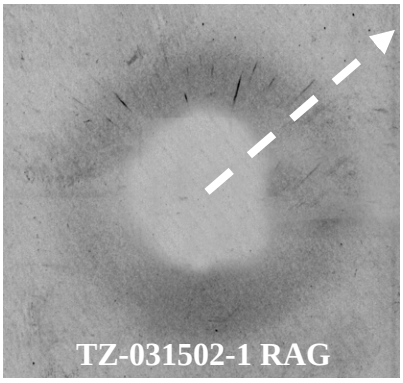

Figure 1: *Inverted image of a typical transmission diffraction pattern from a RAG sample obtained with a synchrotron white-beam source. Dashed white arrow shows where typical line profile is taken.*

An example of a typical exposed Polaroid film for a RAG sample used in transmission mode scattering is shown in Figure 1. All Polaroids obtained from transmission mode scattering experiments showed a classical amorphous structure as indicated by the diffuse ring of scattering seen in the this figure. This demonstrates the amorphous nature of these materials through the entire thickness (up to 2 mm thick). The dashed white arrow indicates where a typical line profile can be taken across the image and converted to a standard "Intensity vs. 2θ" plot, knowing the necessary geometrical parameters such as sample-to-film distance and Polaroid film sizes. Several of these line profiles were constructed for each sample and averaged in order to compare to reflection mode scattering for verification of results.

Reflection Mode Scattering

The scattering results for all reflection mode experiments were converted to $\sin\theta/\lambda$ for comparisons. Additionally, results from the corresponding transmission mode experiments were included (after proper line profile and absorption conversions were performed). Figure 2 shows a representative comparison of the three experimental setups for a RAG sample.

This figure clearly shows the overlap of amorphous peaks at approximately $\sin\theta/\lambda = 0.23$, and also shows the very good agreement between results obtained from the synchrotron and lab sources. One also notes the appearance of an additional peak at approximately $\sin\theta/\lambda = 0.21$ in the synchrotron data, which indicates at least some small amount of crystallinity. This peak is most likely not present in the other data sets because of a lack of resolution. Synchrotron radiation typically has very low divergence which allows for "cleaner" results. The results from the transmission mode experiment are less clear in that the amorphous peak is quite broad and does not follow the shape of the other two data sets. This is an artifact of the line profile and $\sin\theta/\lambda$ conversions which involves the averaging of data over the entire energy range used in this particular white-beam x-ray source (2-40 KeV), which tends to disperse the scattering data.

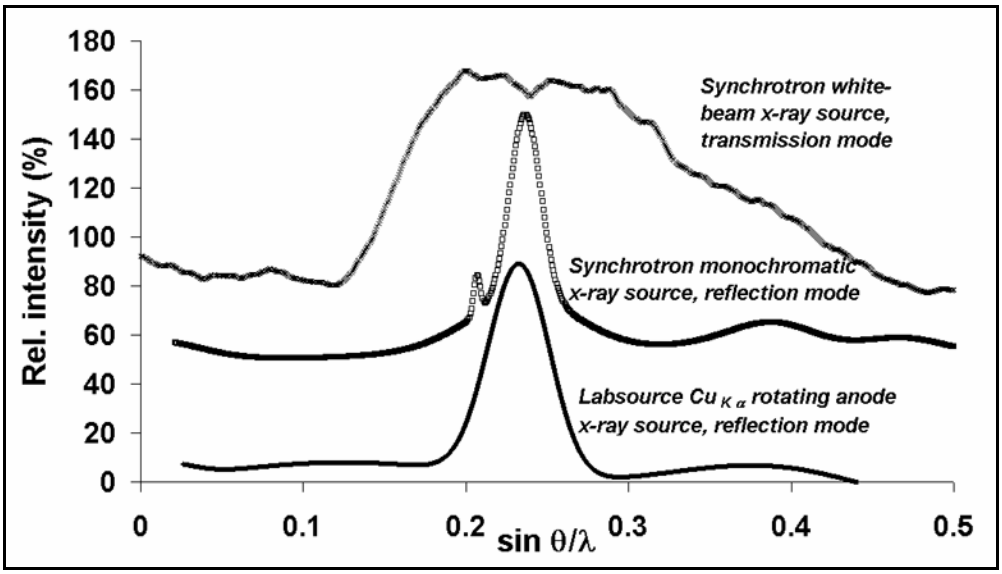

Figure 2: *Diffraction results for typical RAG sample. (This particular graph is that of sample TZ-031502-1). Vertical offsets of 40 are used for clarity. The presence of an additional peak from synchrotron source data is apparent.*

Radial Distribution Analysis

A model Radial Distribution Function (RDF) was constructed for both the Vitreloy-106 standards and the RAG materials. This was done by creating a damped sine curve for each potential pair of constituent atoms based upon a hard-sphere space-filling model. These damped sine curves were weight averaged according to the chemical composition to obtain the final model RDF. The final RDF and reduced RDF for the RAG model are shown in Figure 3. A similar RDF and reduced RDF were also constructed for the model Vitreloy-106 standards.

Error!

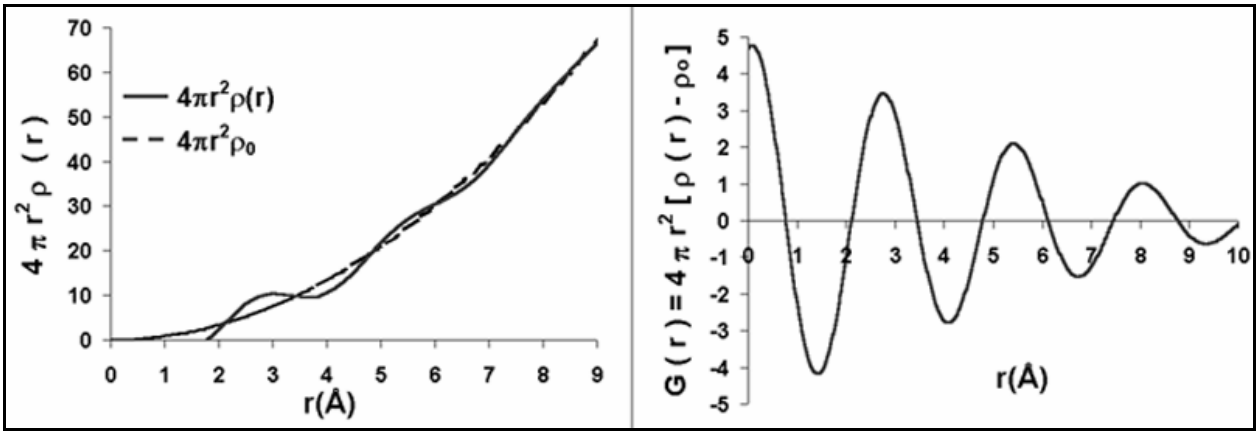

3a **3b**

Figures 3a and 3b: *Model a). RDF (radial distribution function) and b). Reduced RDF, G(r), for $Ni_{60}Nb_{37}Sn_3$ RAG (refractory alloy glass).*

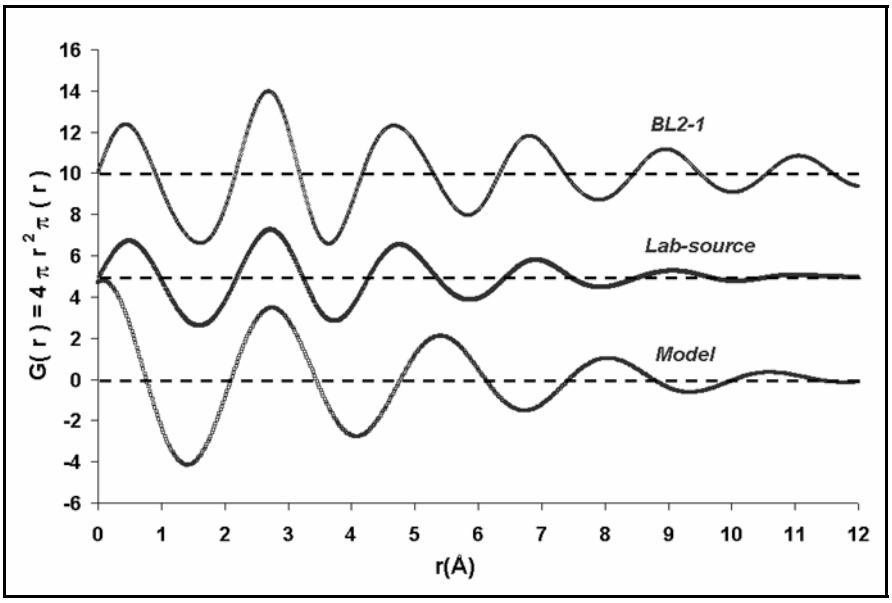

Figure 4: *Reduced RDFs for a typical RAG sample (sample no. 031502-2).*

Table 1: Nearest neighbor information for all Vitreloy-106 samples.
(From lab source data sets)

	1st nearest neighbor		2nd nearest neighbor		3rd nearest neighbor	
	Distance (Å)	**# atoms**	**Distance (Å)**	**# atoms**	**Distance (Å)**	**# atoms**
031502-4 VIT	3.0 ± 0.3	9.4 ± 2.6	5.4 ± 0.3	26.1 ± 2.6	7.8 ± 0.3	50.6 ± 2.6
031502-5 VIT	3.0 ± 0.3	9.4 ± 2.6	5.4 ± 0.3	26.1 ± 2.6	7.8±0.3	50.8 ± 2.6
MODEL	***2.9 ± 0.3***	***10.7 ± 1.2***	***5.84 ± 0.3***	***32.7 ± 1.2***	***8.9 ± 0.3***	***56.0 ± 1.2***

Table 2: Nearest neighbor information for all RAG samples.

	1st nearest neighbor		2nd nearest neighbor		3rd nearest neighbor	
	Distance (Å)	**# atoms**	**Distance (Å)**	**# atoms**	**Distance (Å)**	**# atoms**
031502-1 RAG						
Lab Source	2.7 ± 0.3	10.7 ± 2.6	4.8 ± 0.3	25.9 ± 2.6	6.9 ± 0.3	46.4 ± 2.6
Synchrotron source	2.7 ± 0.3	12.8 ± 2.6	4.6 ± 0.3	28.8 ± 2.6	6.8 ± 0.3	48.0 ± 2.6
031502-2 RAG						
Lab Source	2.7 ± 0.3	10.7 ± 2.6	4.8 ± 0.3	26.1 ± 2.6	6.9 ± 0.3	45.8 ± 2.6
Synchrotron source	2.7 ± 0.3	12.8 ± 2.6	4.7 ± 0.3	28.7 ± 2.6	6.8 ± 0.3	48.6 ± 2.6
MODEL	***2.5 ± 0.3***	***11.5 ± 1.2***	***5.4 ± 0.3***	***33.9 ± 1.2***	***8.0 ± 0.3***	***62.4 ± 1.2***

Experimental scattering data were converted to radial distribution functions following Warren's approximate method for materials of more than kind of atom. These RDFs were further converted to the corresponding *reduced* RDFs using measured values of atomic density. Figure 4 shows the reduced RDFs for a typical RAG sample. A similar RDF and reduced RDF were also constructed for the model Vitreloy-106 standards. Figure 4 does NOT include error bars for the sake of clarity, but the salient results for all Vitreloy-106 and RAG samples are summarized in Tables 1 and 2.

While the figures indicate average experimental nearest neighbor distances smaller than the model, the tables make it apparent that the experimental results mostly agree with the model within the margin of experimental error.

Although the results presented here show a fundamental agreement with the RDFs based upon hard-sphere modeling, further refinements are needed, including a better estimate of experimental errors.

CONCLUSIONS

Several important contributions to the understanding of the structure of refractory alloy glasses, specifically $Ni_{60}Nb_{37}Sn_{3,}$ have been made. First, it was found that these materials are amorphous throughout their thickness of 2 mm. This is a significant complement to the existing reflection mode scattering that has been performed on bulk metallic glasses. Additionally line profiles across the two-dimensional diffraction patterns from these experiments could be correlated quite well with reflection mode diffraction results.

Models for both Vitreloy-106 and $Ni_{60}Nb_{37}Sn_3$ were constructed and their corresponding total, and reduced, radial distribution functions were compared to those obtained from experimental data. The experimental reduced radial distribution functions were shown to agree with those of the corresponding model for the first two nearest neighbors.

ACKNOWLEDGEMENTS

This work was supported by DARPA, Department of Defense contract number DAAD 19-01-0525 through California Institute of Technology and Department of Energy for research performed at the Stanford Synchrotron Radiation Laboratory. The authors of this paper would also like to acknowledge W. L. Johnson, D. Xu and H. Choi-Yim at California Institute of Technology for providing test samples.

REFERENCES

1. W.L. Johnson, S.J. Poon, J. Durand and Pol Duwez, *Phys. Rev.* **B18** (1978) p 206.
2. Pol Duwez, R. H. Willens and R. C. Crewdson, *J. Appl. Phys*. **36** (1965) p 2267.
3. A. Peker and W. L. Johnson, *Appl. Phys. Lett*. **63**, 17, (1993), p 2342.
4. A. Masuhr, T. A. Waniuk, R. Busch, and W.L. Johnson, *Phys Rev. Lett.* **82**, 11, (1999) p 2290
5. H. Choi-Yim, D. Xu, W. L. Johnson, submitted to *Applied Physics Letters* 10/4/02
6. B. E. Warren, "X-ray Diffraction", p 116-142 (1969)
7. V. Petkov, *J. Appl. Cryst*. **22**, 387, (1989)